Supplementary Figure 1

a

Lines	Genotype	Background	Clinical information	Reference
Control	*Wt/Wt*	Fibroblast + Episomal	Population/Sex: Caucasian / F	Okita et al[1]
FUS[H517D/H517D]	H517D/H517D	Control + TALEN	Age at fibroblast donation: 36 y.o.	Ichiyanagi et al[4]
FUS[Rescued]	*Wt/Wt*	*FUS*-ALS + TALEN	Population/Sex: Asian / M	This study
FUS-ALS	*Wt/H517D*	Fibroblast + Episomal	Age at fibroblast donation: 43 y.o. Disease onset: Cervical area at 41 y.o.	Ichiyanagi et al[4]

b
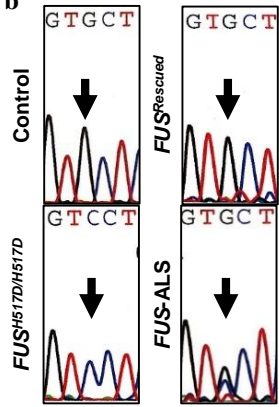
c
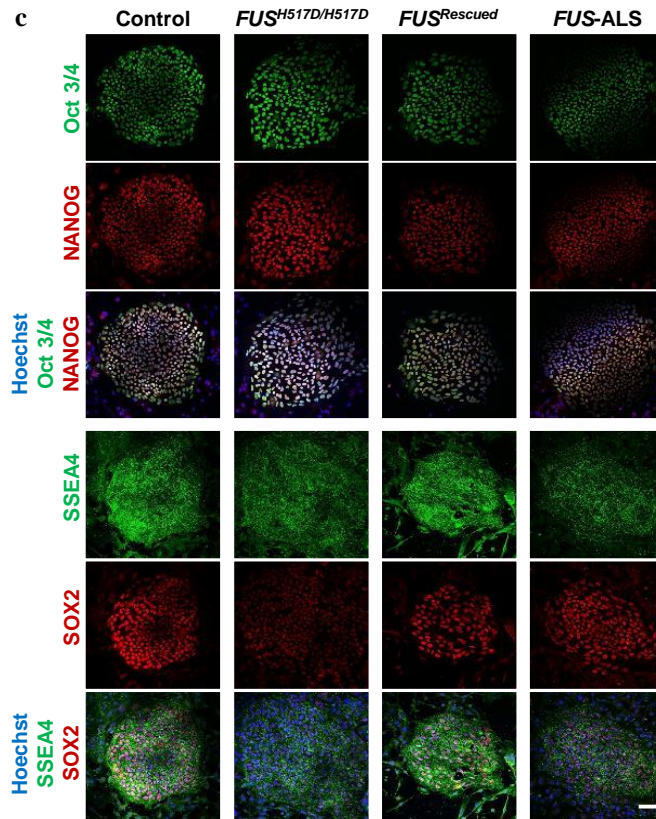
d
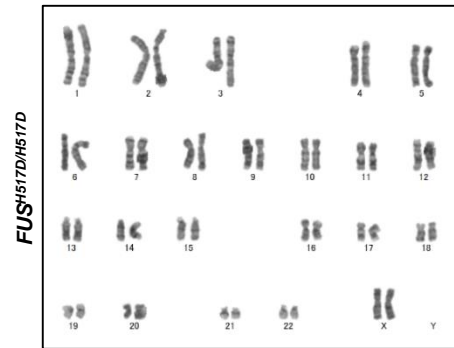
e
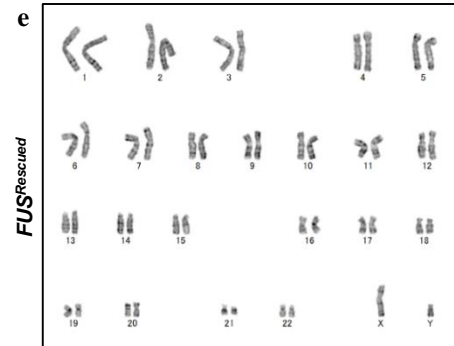
f
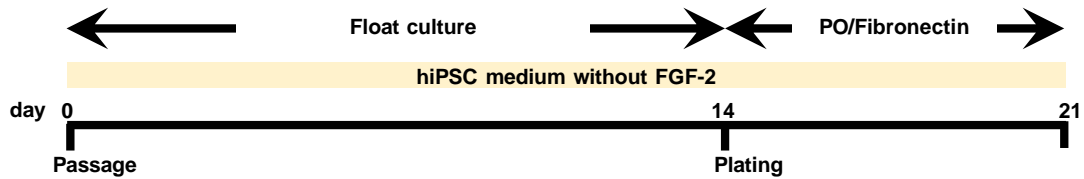
**g**
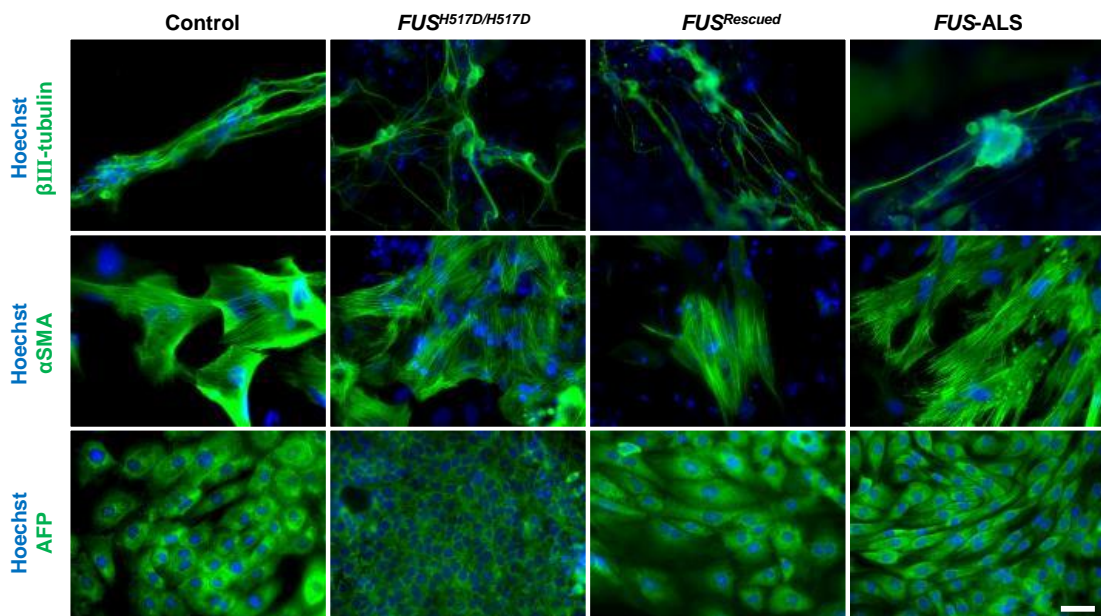
Supplementary Fig. 1. hiPSC quality check.

(a) The hiPSC lines used in the present study. (b) Direct sequencing results for each hiPSC line. Control and $FUS^{Rescued}$ lines contain wild-type sequences. The FUS-ALS line contains a hetero-mutation, whereas the $FUS^{H517D/H517D}$ has a homo-mutation. The objective base is represented by an arrow. (c) Representative ICC results of the pluripotency markers. Bar; 100 μm. (d,e) The normal karyotypes were confirmed in both of the genome-edited lines. (f,g) The differentiation potentials were checked for all lines. f; The hiPSCs were cultured for 3 weeks as shown in the schema (also refer to the Materials and methods section). g; The hiPSCs were confirmed to exhibit the markers of three germ layers (i.e., ectoderm: βIII-tubulin, mesoderm: αSMA, endoderm: AFP). Bar: 50 μm.

Supplementary Figure 2
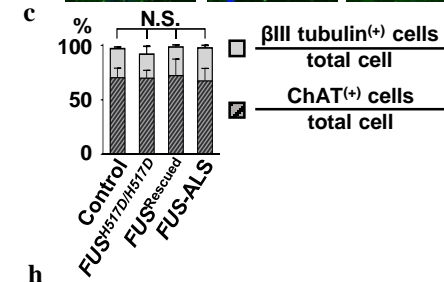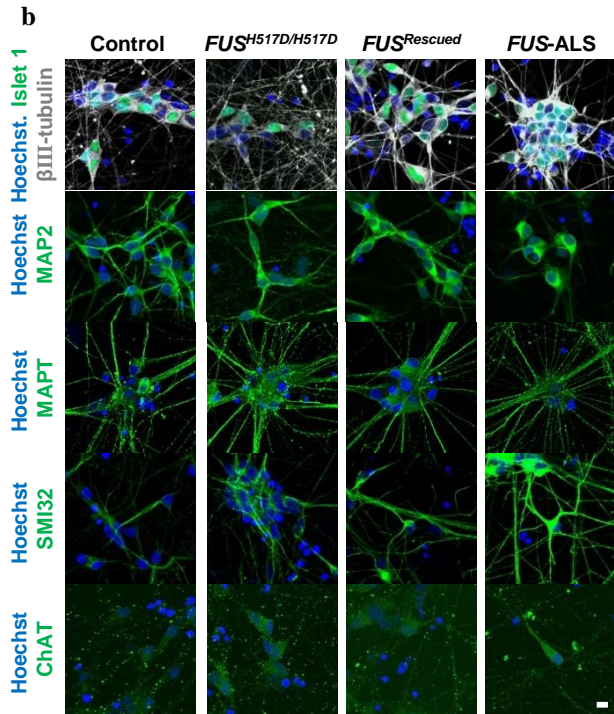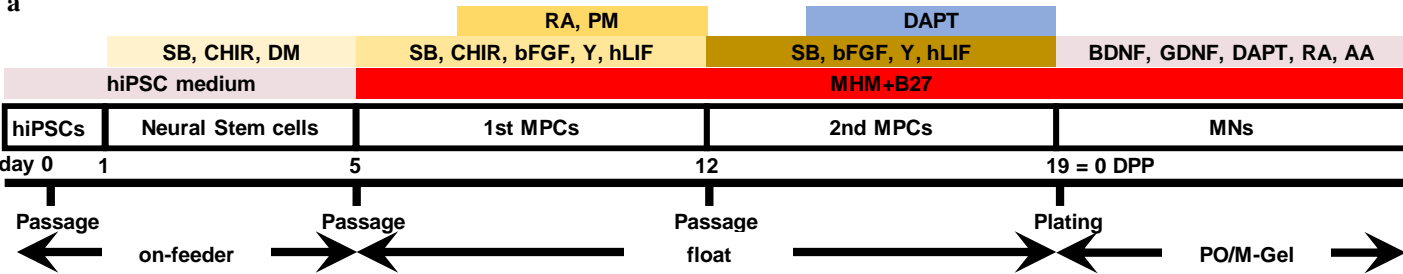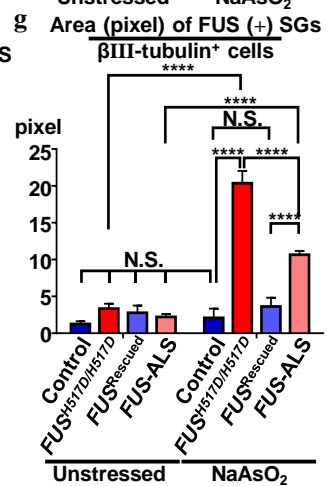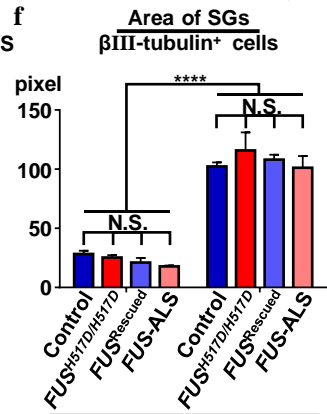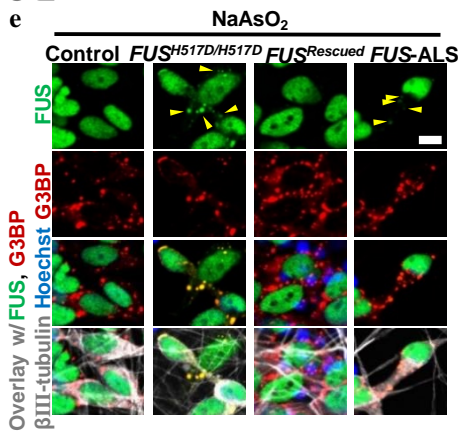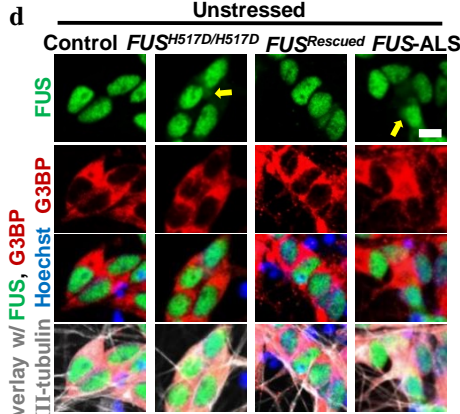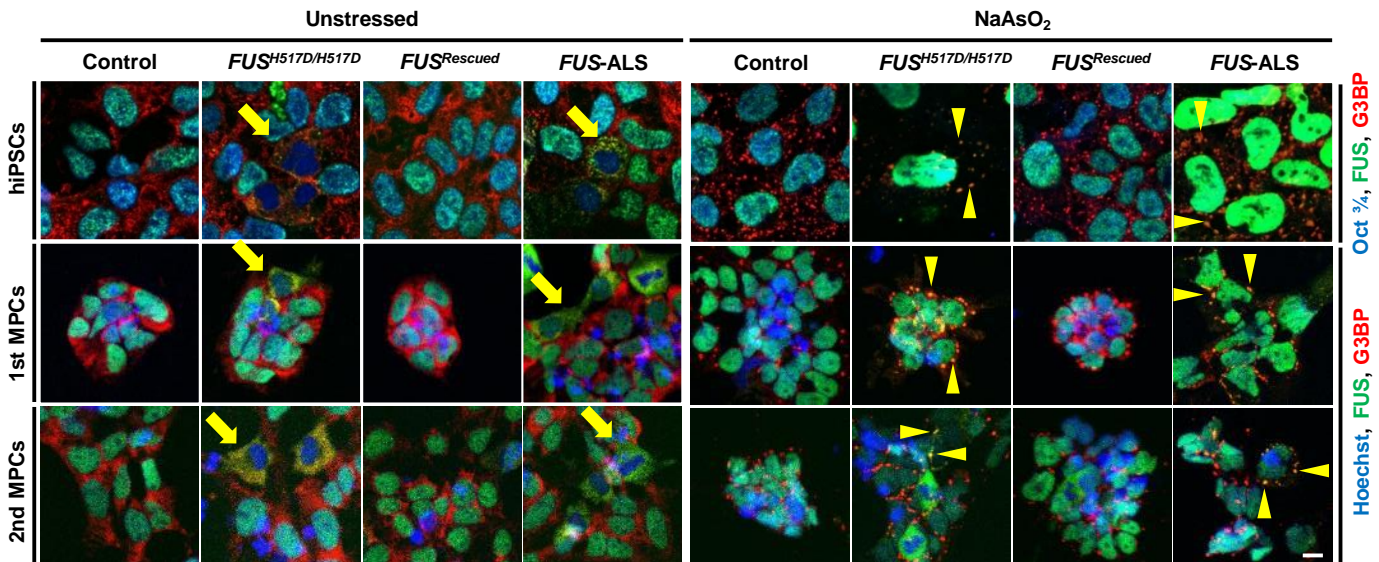
Supplementary Fig. 2. MN differentiation: Mutant FUS mis-localizations in various cell types including hiPSC-derived MNs.

(a) The schema of the MN induction method. MNs are plated at 0 DPP. The abbreviations of chemical compounds used are as follows. MHM, medium hormone mix (refer to previous report [43]); CHIR, CHIR99021; DM, dorsomorphin; SB, SB431541; PM, purmorphamine; hLIF, human recombinant leukemia inhibitory factor protein; BDNF, human recombinant brain-derived neurotrophic factor; GDNF, human recombinant glial-cell-derived neurotrophic factor; RA, retinoic acid; AA, ascorbic acid. The medium used for MN culture is defined as MN medium. (b) Representative ICC images of (motor) neuronal markers. MNs at 10 DPP were stained. Bar; 10 µm. (c) Induction efficiency was analyzed using Cellomics by counting βIII-tubulin with/without ChAT positive cells. N = 3, independent experiments in triplicate, with >4,000 cells/experiment analyzed using two-way ANOVA. (d) Representative images of hiPSC-derived MNs at 10 DPP under unstressed conditions. The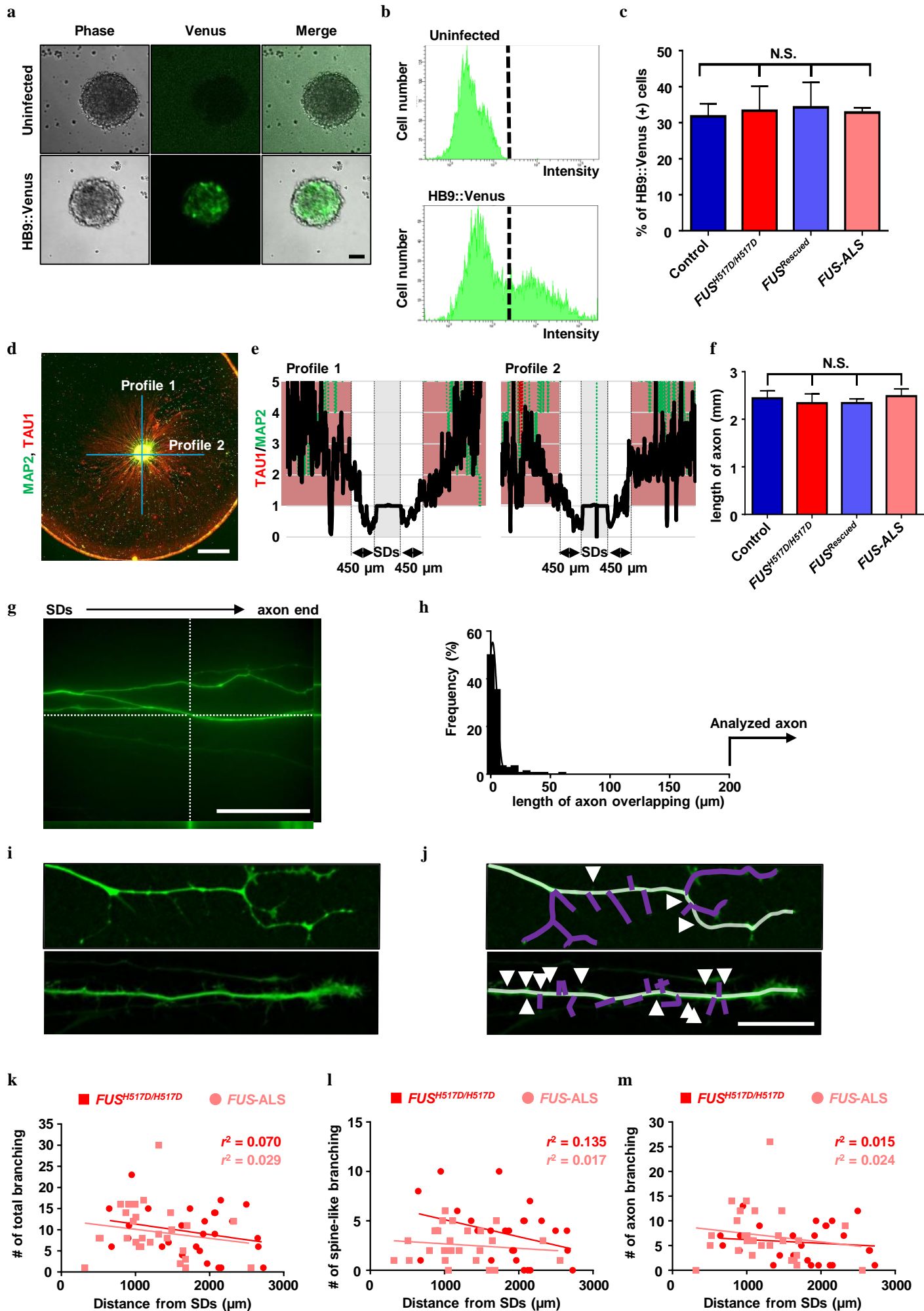 WT-FUS (Control and $FUS^{Rescued}$; green) was found to be localized to the nucleus. However, FUS was localized to the cytoplasm in FUS-mutant lines (yellow arrows). (e) With 1 mM $NaAsO_2$ treatment for 30 min, G3BP (red)-positive SGs were formed in all cell lines. The cytoplasmic FUS of the FUS-mutant lines co-localized with G3BP (yellow arrowheads), whereas WT-FUS was not co-localized. Bar: 10 µm. (f) Quantification of cytoplasmic SGs with the Cellomics scan. No differences in SGs among the cell lines were observed. (g) Quantification of cytoplasmic FUS-positive SGs with the Cellomics scan. Abnormal accumulation of FUS was significantly increased in FUS-mutant lines. N = 3, independent experiments with triplication of each experiment, with >10,000 cells/experiment analyzed using two-way ANOVA. (h) The mutant FUS mislocalized (yellow arrows) and co-localized with G3BP (yellow arrowheads) under 1 mM $NaAsO_2$ treatment for 30 min in hiPSCs and MPCs stages. Bar: 10 µm.

Supplementary Figure 3

a

	Phase	Venus	Merge
Uninfected			
HB9::Venus			

b

Uninfected

Cell number — Intensity

HB9::Venus

Cell number — Intensity

c

% of HB9::Venus (+) cells

N.S.

Control $FUS^{H517D/H517D}$ $FUS^{Rescued}$ FUS-ALS

d

MAP2, TAU1

Profile 1

Profile 2

e

Profile 1

TAU1/MAP2

SDs
450 μm 450 μm

Profile 2

SDs
450 μm 450 μm

f

length of axon (mm)

N.S.

Control $FUS^{H517D/H517D}$ $FUS^{Rescued}$ FUS-ALS

g

SDs → axon end

h

Frequency (%)

Analyzed axon

length of axon overlapping (μm)

i

j

k

$FUS^{H517D/H517D}$ FUS-ALS

# of total branching

r^2 = 0.070
r^2 = 0.029

Distance from SDs (μm)

l

$FUS^{H517D/H517D}$ FUS-ALS

# of spine-like branching

r^2 = 0.135
r^2 = 0.017

Distance from SDs (μm)

m

$FUS^{H517D/H517D}$ FUS-ALS

# of axon branching

r^2 = 0.015
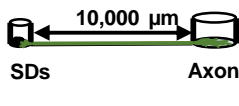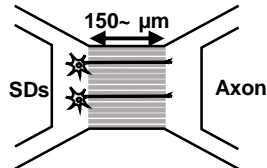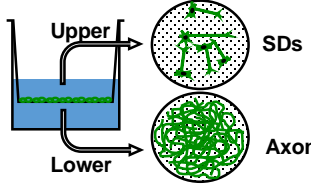r^2 = 0.024

Distance from SDs (μm)

Supplementary Fig. 3. Cultured MPC profiles and counting method for MN axons.

(a) Venus-positive cells were detected at 0 DPP. Bar = 50 µm. (b) The % of Venus-positive cells were analyzed using FACS. Venus-positive cells were defined when the intensity was higher than the cut off (black dotted line). (c) The % of Venus-positive cells from each line. There were no differences in the proportion of these cells between each line. N = 3 independent experiments analyzed using one-way ANOVA. (d,e) TAU1/ MAP2 intensities changed from < 1 to > 1 at approximately 450 µm from the SDs. d: The ICC image is the same as Fig. 1c. Bar = 1 mm. The line profiles were analyzed in (e). (e) The red dot lines represent the intensity of TAU1, the green dot lines represent the intensity of TAU1, and the black lines represent TAU1/MAP2. (f) The axon length did not differ with the presence of the *FUS* mutation. The longest three axon lengths were analyzed at 10 DPP from three independent experiments using one-way ANOVA. (g,h) The analyzed axon. g; Orthogonal image of axon overlapping. Unfortunately, the overlapping was indistinct. Bar; 50 µm. The axon elongated from the left side of the image. h; The histogram represents the length of the overlapping axon. Over 100 crossing points were analyzed and no axons were merged > 80 µm. Because we analyzed 200 µm of the axon end, there was no possibility that the axon end included multiple axons. (i) Representative images of the axon end with branching (one of the images is the same as Fig. 1d). (j) The axon branches were classified as two types. At first, the main flow of the axon was defined as the longest neurite in the axon end (white line). Subsequently, the spine-like branching was defined as branching that diverged from the main flow at least 0.5 µm and was shorter than 2 µm (white arrow heads). Axon branching was defined as branches >2 µm (purple lines). Branching from the counted flow was not counted. The 150 µm of the axon ends, excluding the growth cone (defined as the 50 µm of axon end), represented the region of interest for counting. Bar; 50 µm. (k–m) There was no relationship between branching and axon length. Scatter chart with the number of axon branching and the axon length, as well as the correlation coefficient (r^2). The red circle and pink square represent $FUS^{H517D/H517D}$ and *FUS*-ALS, respectively.
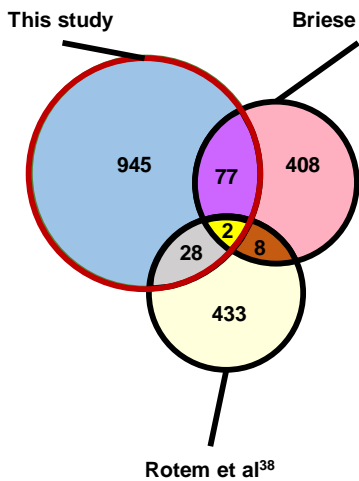
a

Reference	This study	Briese et al[19]	Bigler et al[68]	Nijssen et al[39]	Rotem et al[38]	Maciel et al[37]
Device	Nerve organoid device	Microfluidic chamber			Modified Boyden	
Company	Jiksak Bioengineering	Xona Microfluidics			Corning	
Dimension	3D	2D			2D	
Used cell	hiPSCs-MN	Primary mouse MN	hESC-neuron	A. mESCs-MN B. hiPSCs-MN	Primary mouse MN	hiPSCs-MN ChAT(+) 65%
Cell number	10^4~	10^6	5×10^3	A. 5×10^5 B. 1.5×10^5	5×10^5	2×10^6
Neurite length (μm)	10,000~	150~			No data	
Pore size (μm)	150	3			1	
RNA	12 ng (1 ng/μl) ~	20 pg~	10 pg (2 pg/μl)	No data	0.3 ng/μl	80~100 ng
Scheme	10,000 μm SDs ↔ Axon	150~ μm SDs ↔ Axon			Upper → SDs Lower → Axon	

b

SDs enriched genes

This study — Briese et al[19] — Rotem et al[38]

945 | 77 | 408 | 28 | 2 | 8 | 433

c

Axon enriched genes

This study — Briese et al[19] — Rotem et al[38]

738 | 58 | 239 | 82 | 6 | 86 | 1446

d

This study — Briese et al[19] — Rotem et al[38] — Nijssen et al[39]

655 | 190 | 45 | 49 | 70 | 3 | 13 | 1103 | 1826 | 3 | 51 | 35 | 12 | 83 | 343
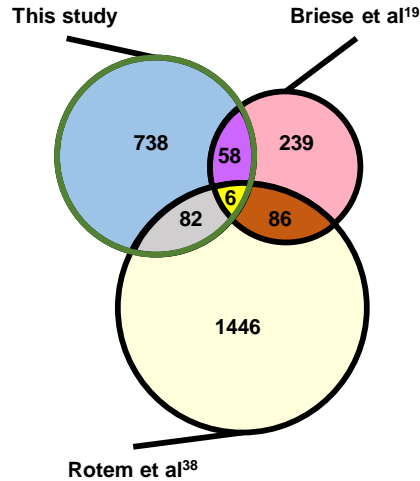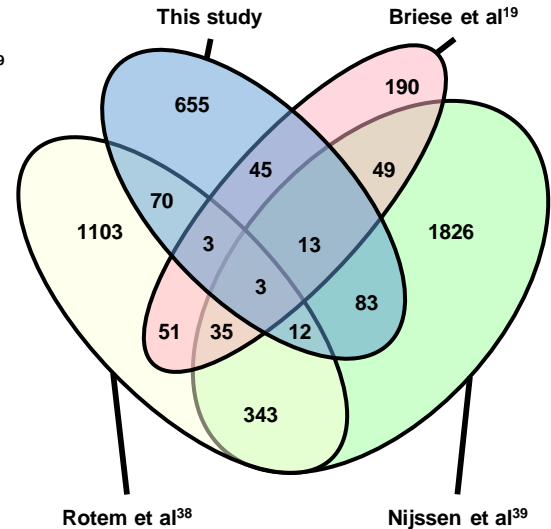
Supplementary Fig. 4. MN differentiation. Mutant FUS mis-localizations in various cell types including hiPSC-derived MNs.

(a) Schema of the differences in microfluidic devices for analyzing the axon fraction [19, 37-39, 68]. (b,c) Comparison of the SDs and axonal RNA profiles in the present study with two previous reports, which used MNs and reported SDs and provided axon-enriched gene lists. We used the gene lists from Rotem et al. and Briese et al. Some genes were disregarded based on methodological differences. (d) Comparison of axon-enriched genes [presented at (c)] with axon-detected (not axon-enriched) genes that were reported in Nijssen et al.
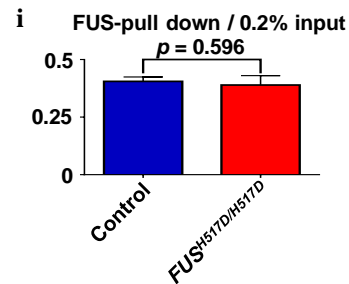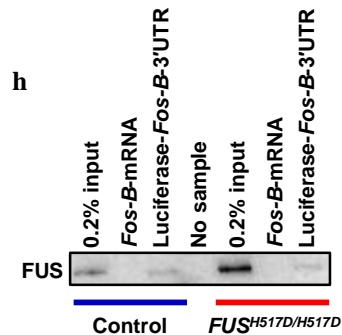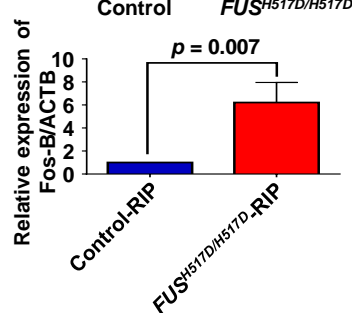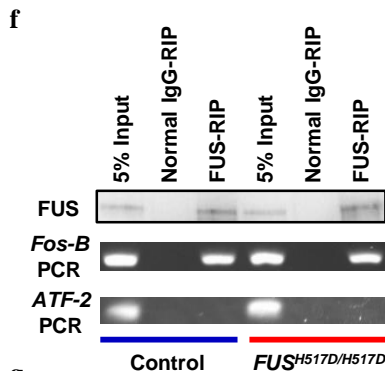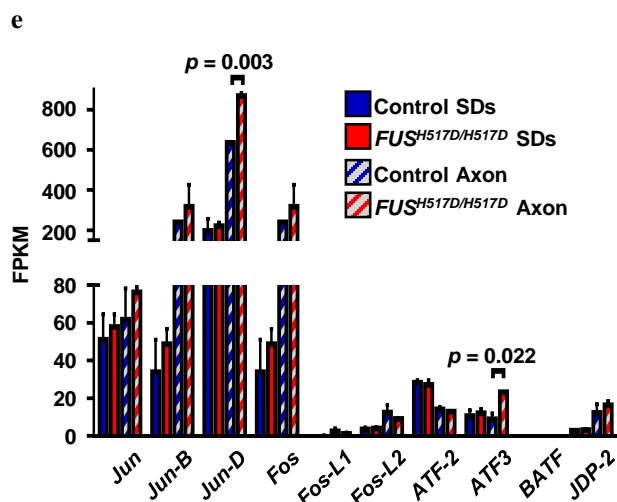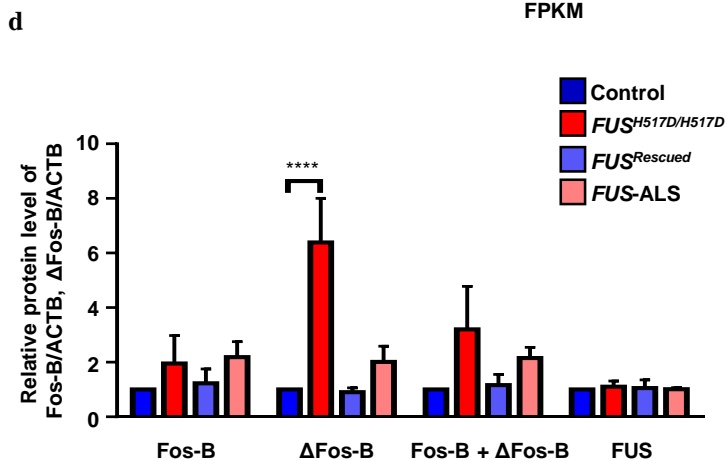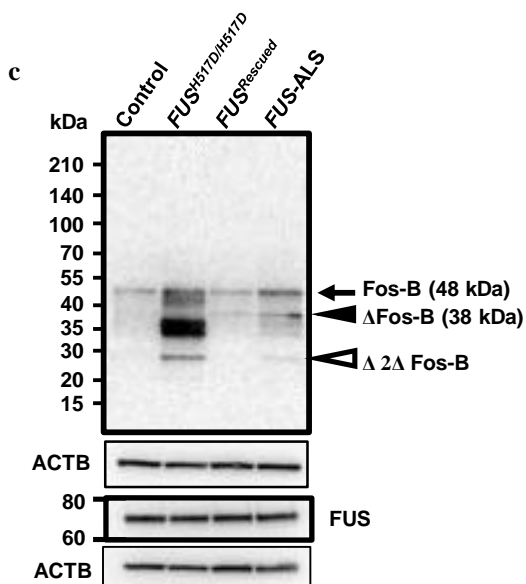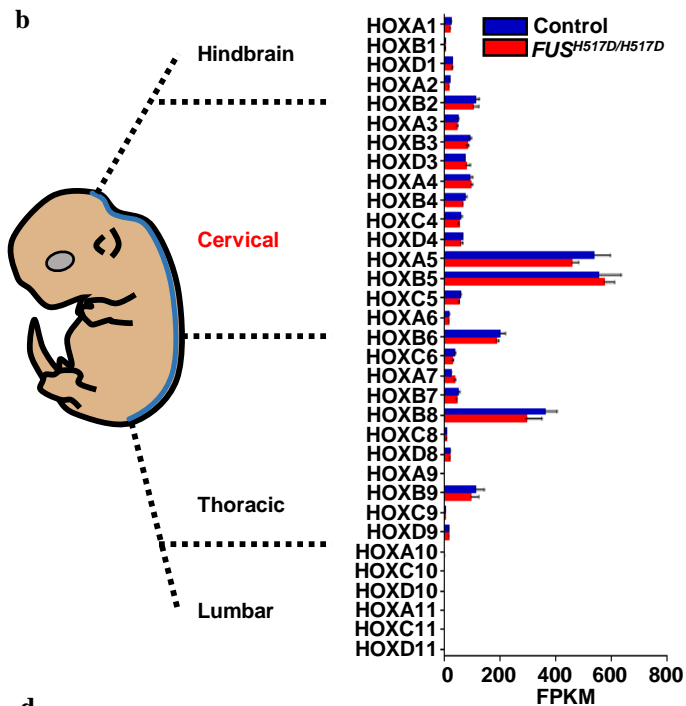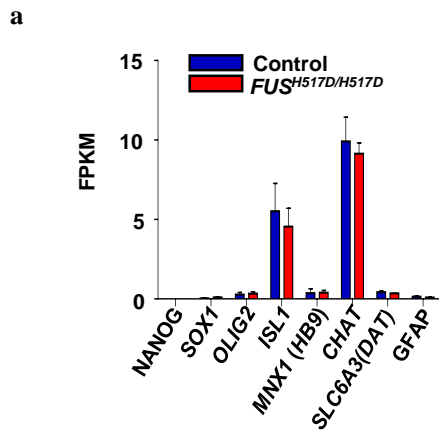
Supplementary Fig. 5. Upper cervical spinal matured MNs with or without *FUS* mutation were compared in RNA-seq.

(a,b) Upper cervical spinal matured MNs were analyzed using RNA-seq. The maturity and schema of the depicted expression patterns of the chromosomally linked Hox genes along the rostro-caudal axis are shown based on previous reports [46, 47]. The Control and the isogenic lines $FUS^{H517D/H517D}$ hiPSC-derived MNs were compared. Each line showed matured cervical MN RNA expression. Low expression levels of GFAP and DAT indicated astrocyte or dopaminergic neurons that were not differentiated in this protocol. (c) The immunoblot of Fos-B and FUS from entire MNs at 10 DPP. Fos-B and the variants [delta-Fos-B (ΔFos-B) and delta-2-delta-Fos-B (Δ2ΔFos-B)] are upregulated with *FUS*-mutant lines. There are no differences in FUS expression levels among the four cell lines. (d) Relative protein expression levels of control sample are presented. Fos-B and FUS levels adjusted with ACTB level in each of the samples. N = 3 from three independent experiments were analyzed using one-way ANOVA. (e) FPKM data with AP-1 related genes in RNA-seq results. The Control FPKM was compared with $FUS^{H517D/H517D}$ sample using Student's *t*-test with each fraction. (f) RIP from the Control and $FUS^{H517D/H517D}$ samples. FUS proteins were precipitated from both samples (upper figure). *Fos-B* mRNA was precipitated from the Control and $FUS^{H517D/H517D}$ samples (middle figure), whereas *ATF-2* were not (lower figure). (g) qRT–PCR result for RIP samples from the Control and $FUS^{H517D/H517D}$. Because *ACTB* were detected from RIP samples, *ACTB* were used for the control. Expression levels of *Fos-B* mRNA relative to the Control samples are presented. N = 3 independent experiments were analyzed by Student's *t*-test. (h) RNA pulldown assay from the Control and $FUS^{H517D/H517D}$ samples. FUS was detected from *Fos-B* 3'UTR biotinylated RNA without differences between both samples. (i) The quantification of FUS protein levels in RNA pulldown assay. N = 3 independent experiments were analyzed by Student's *t*-test.

Supplementary Figure 6

a

Microgrooves
450 μm

SDs

Axon

SDs side ← 450 μm → Axon side

|c| SDs compartment
|d| Groove end to check growth cone area
|e| Axon compartment

→ Supplementary Figure 6c–e

b

| Phalloidin / Actin | smFISH | Merge |

No probe

Anti-Fos-B

c

| Phalloidin / Actin | smFISH-Fos-B | smFISH-Fos-B, Hoechst | Merge |

SDs

Control

$FUS^{H517D/H517D}$

f

p = 0.0006

Relative *Fos-B* luminance / cell

Control $FUS^{H517D/H517D}$

d

Growth cone

Control

$FUS^{H517D/H517D}$

← Micro groove

Device (barrier)

*

*

g

p = 0.019

Relative luminance / ROI (*)

Control $FUS^{H517D/H517D}$

e

Axon

Control

$FUS^{H517D/H517D}$

h

p = 0.0006

Relative luminance / Phalloidin
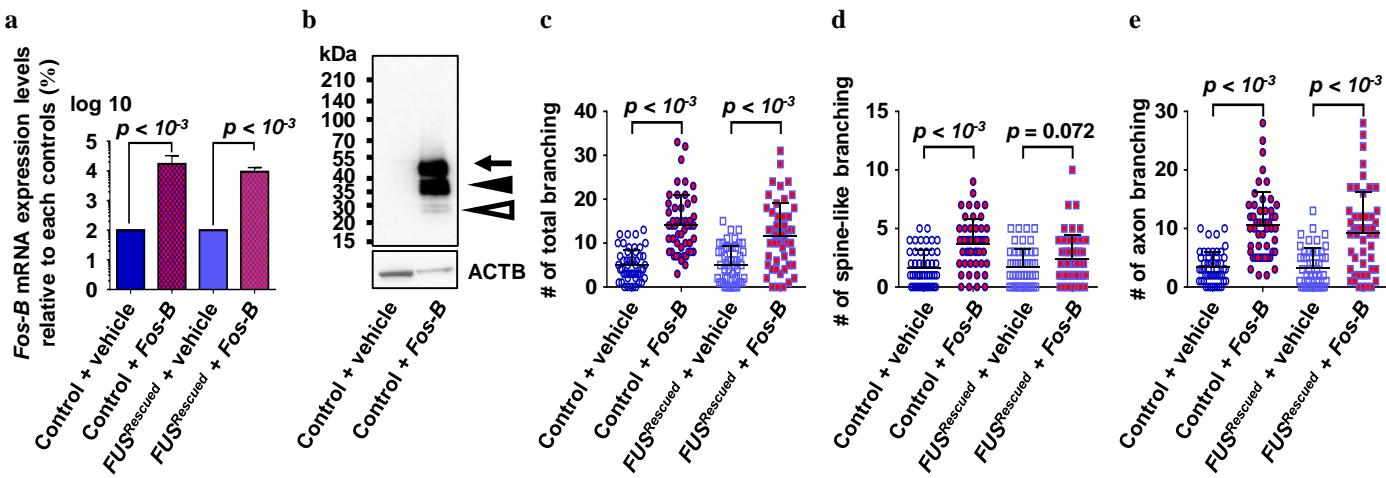
Control $FUS^{H517D/H517D}$

Supplementary Fig. 6. *Fos-B* upregulation was confirmed in *FUS*-mutants using smFISH.

(a) The schema of using smFISH for analyzing the SDs, growth cones, and axons. The microfluidics used in this figure are appropriate for analyzing single axons. The device could divide axons because the SDs unable to pass the microfluidics, which are 450 µm in length. (b) Comparison of no-probe negative control and the smFISH staining at axon fraction (same fraction with Supplementary Fig. 6e) with *FUS*$^{H517D/H517D}$ hiPSC-derived MNs at 10 DPP on microfluidics. Compared to no-probe negative control (upper figures), the signals of smFISH for *Fos-B* mRNA were observed on the phalloidin-positive cell structures (lower figures). (c) Representative images of smFISH for *Fos-B* at the SDs. Bar = 50 µm. (d) Representative images of smFISH for *Fos-B* at the growth cone. White arrow represents one of the microgrooves via which axons could pass. White dotted lines represent the barrier of the device via which no cell or fluids could pass. Bar = 50 µm. (e) Representative images of smFISH for *Fos-B* at the axons. Bar = 50 µm. (f–h) Quantification of *Fos-B* smFISH luminance for each fraction. f: smFISH luminance at the SDs were normalized with the cytoplasmic area. N = 5. Student's *t*-test. g: smFISH luminance at the growth cone was normalized using the luminance from the region of interests [referred by white square with asterisk at (d)] where no cells or fluid are present. N = 3. Student's *t*-test. h: smFISH luminance at the axon was normalized using the luminance of phalloidin. N = 3. Student's *t*-test. In all fractions, the fluorescence of smFISH (for *Fos-B*) was higher in the *FUS*$^{H517D/H517D}$ line. However, we could not confirm the characteristic localization of *Fos-B* mRNA.
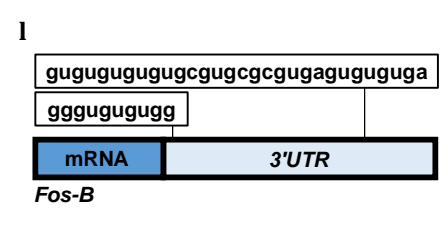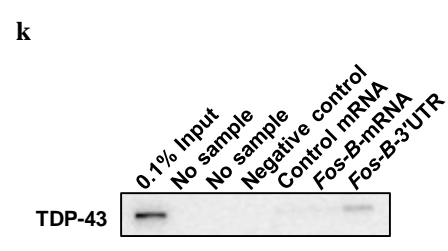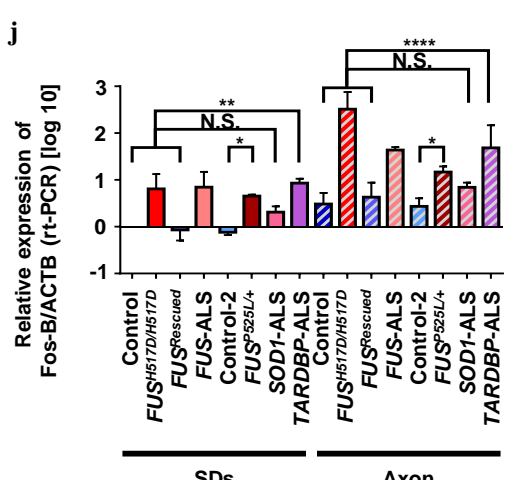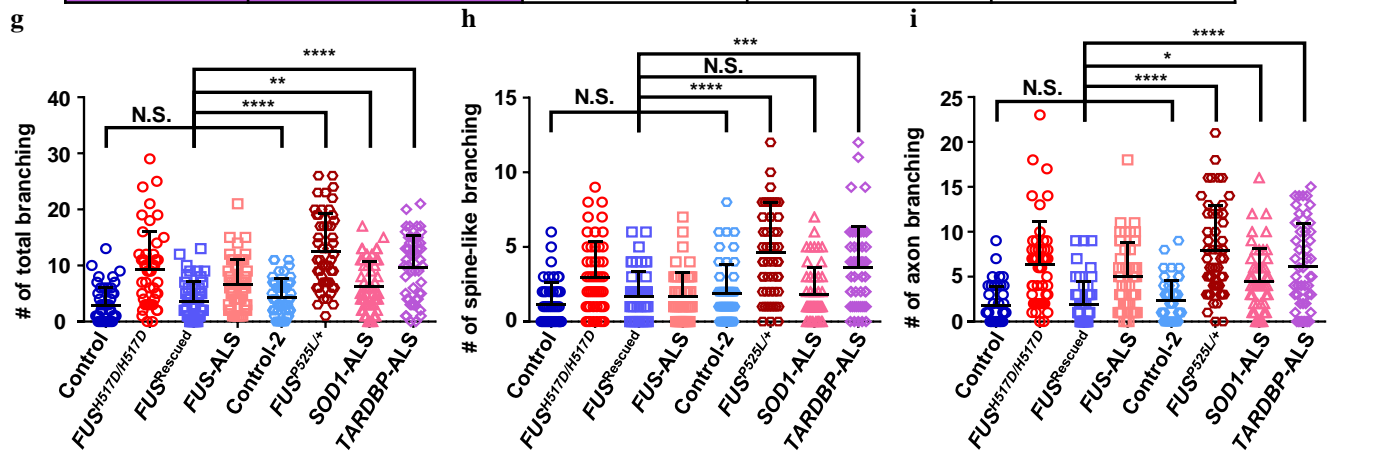
Supplementary Figure 7

Fos-B overexpression

a

Fos-B mRNA expression levels relative to each controls (%) — log 10

$p < 10^{-3}$ $p < 10^{-3}$

Control + vehicle / Control + *Fos-B* / $FUS^{Rescued}$ + vehicle / $FUS^{Rescued}$ + *Fos-B*

b

kDa: 210, 140, 100, 70, 55, 40, 35, 30, 25, 15

ACTB

Control + vehicle / Control + *Fos-B*

c

# of total branching

$p < 10^{-3}$ $p < 10^{-3}$

Control + vehicle / Control + *Fos-B* / $FUS^{Rescued}$ + vehicle / $FUS^{Rescued}$ + *Fos-B*

d

# of spine-like branching

$p < 10^{-3}$ $p = 0.072$

Control + vehicle / Control + *Fos-B* / $FUS^{Rescued}$ + vehicle / $FUS^{Rescued}$ + *Fos-B*

e

# of axon branching

$p < 10^{-3}$ $p < 10^{-3}$

Control + vehicle / Control + *Fos-B* / $FUS^{Rescued}$ + vehicle / $FUS^{Rescued}$ + *Fos-B*

f

Lines	Genotype	Background	Clinical information	Reference
Control-2	Fibroblast + Lentivirus	Caucasian / F, 36 y.o.	*Wt/Wt*	Takahashi et al[2]
$FUS^{P525L/+}$	Control-2 + CRISPR		*Wt/P525L*	This study
SOD1-ALS	PBMC + Episomal	Asian / F, 37 y.o.,	*Wt/H46R*	Fujimori et al[5]
TARDBP-ALS	Fibroblast + Episomal	Asian / F, 62 y.o.,	*Wt/M337V*	Egawa et al[6]

g

# of total branching

N.S.   ****   **   ****

Control / $FUS^{H517D/H517D}$ / $FUS^{Rescued}$ / FUS-ALS / Control-2 / $FUS^{P525L/+}$ / SOD1-ALS / TARDBP-ALS

h

# of spine-like branching

N.S.   ****   N.S.   ***

Control / $FUS^{H517D/H517D}$ / $FUS^{Rescued}$ / FUS-ALS / Control-2 / $FUS^{P525L/+}$ / SOD1-ALS / TARDBP-ALS

i

# of axon branching

N.S.   ****   *   ****

Control / $FUS^{H517D/H517D}$ / $FUS^{Rescued}$ / FUS-ALS / Control-2 / $FUS^{P525L/+}$ / SOD1-ALS / TARDBP-ALS

j

Relative expression of Fos-B/ACTB (rt-PCR) [log 10]

N.S.   **   *   ****   N.S.   *

Control / $FUS^{H517D/H517D}$ / $FUS^{Rescued}$ / FUS-ALS / Control-2 / $FUS^{P525L/+}$ / SOD1-ALS / TARDBP-ALS (SDs)

Control / $FUS^{H517D/H517D}$ / $FUS^{Rescued}$ / FUS-ALS / Control-2 / $FUS^{P525L/+}$ / SOD1-ALS / TARDBP-ALS (Axon)

SDs   Axon

k

TDP-43

0.1% Input / No sample / No sample / Negative control / Control mRNA / *Fos-B*-mRNA / *Fos-B*-3'UTR

l

gugugugugugcgugcgcgugaguguguga

gggugugugg

| mRNA | 3'UTR |

Fos-B

m

Lines	Branch	*Fos-B*
Control	→	→
$FUS^{H517D/H517D}$	↑↑	↑↑
$FUS^{Rescued}$	→	→
FUS-ALS	↑	↑
Control-2	→	→
$FUS^{P525L/+}$	↑↑	↑
SOD1-ALS	↑	→
TARDBP-ALS	↑↑	↑

Supplementary Fig. 7. *Fos-B* regulated axon branching may share common mechanisms.
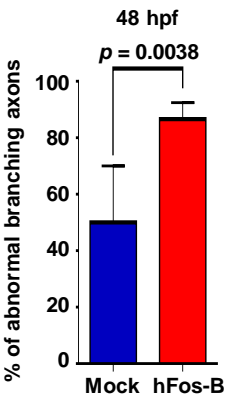
(a–e) Abnormal increases in axon branching was confirmed with *EF-1α::Fos-B* lentivirus co-infection

(with *HB9^{e438}::Venus*). (a) RNA expression levels were confirmed using qRT–PCR [the relative

expression of control (with the ΔΔCt method) is presented; N = 3 independent experiments; Student's *t*-

test]. (b) Immunoblot data from Control hiPSC-derived MNs at 10 DPP with or without Fos-B

overexpression. Abundant amounts of Fos-B, with multiple Fos-B variants, are expressed in the Fos-B

expression lentivirus infection. Black arrow represents Fos-B (48 kDa), black arrowhead represents ΔFos-

B (38 kDa), and white arrowhead represents Δ2ΔFosb as shown in Supplementary Fig. 5c. (c–e);

Quantification of axon branching. Analyzed by Student's *t*-test. Axon branching was increased by *Fosb*

expression. (f) The hiPSC lines used for analyzing extra familial ALS cases. (g–i) Abnormal increases in

axon branching were confirmed in *FUS$^{P525L/+}$*-, *SOD1*-, and *TARDBP*-mutated MNs. To compare with the

control and p.H517D *FUS*-mutant lines, data from Fig. 1e–g are presented and analyzed using one-way

ANOVA. (j) The *Fos-B* expression levels obtained using qRT–PCR from each MN. The expression levels

were normalized to the *Fos-B* expression levels of control SDs using the ΔΔCt method. Although there

were abnormal increases in *Fos-B* expression with *FUS$^{P525L/+}$*- and *TARDBP*-MNs, significant differences

were not observed in *SOD1*-MNs. N = 3 independent experiments; analyzed using one-way ANOVA. (k)

The TDP-43 protein precipitated with the biotinylated *Fos-B* 3′UTR sequence. (l) The schema shows the

site of the TDP-43 binding sequence [69] on *Fos-B*. Compared with *Fos-B* mRNA that includes no

binding sequence, the 3′UTR sequence contains two sites. (m) The inventory of axon branching and *Fos-*

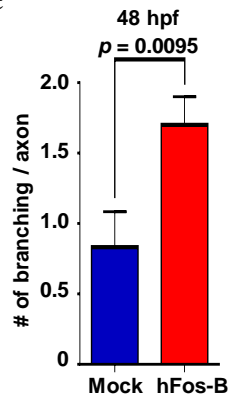*B* upregulation with three ALS-causing mutations.
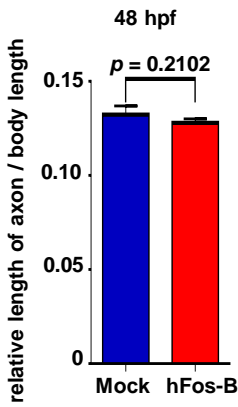
Supplementary Figure 8

a

b

48 hpf

p = 0.0038

% of abnormal branching axons

Mock   hFos-B

c

48 hpf

p = 0.0095

# of branching / axon

Mock   hFos-B

d

48 hpf

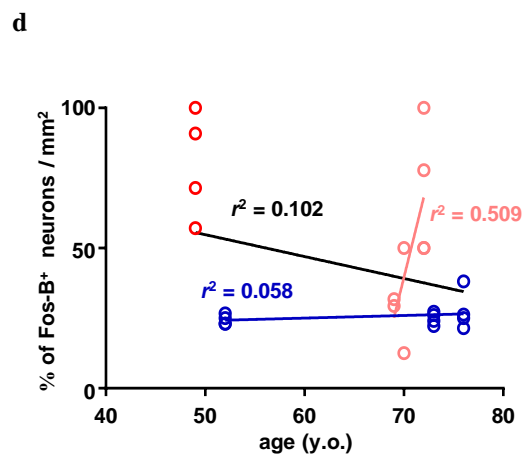*p* = 0.2102

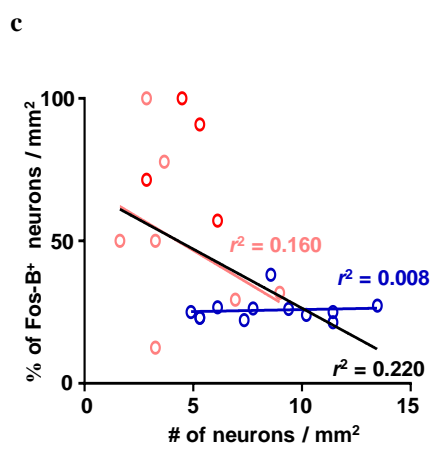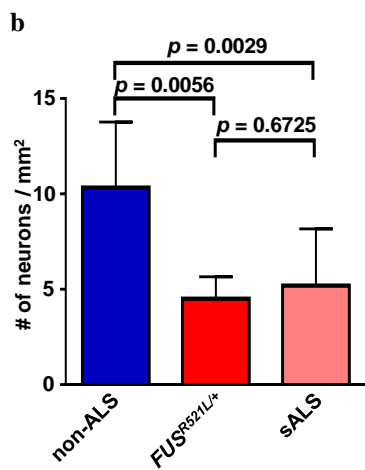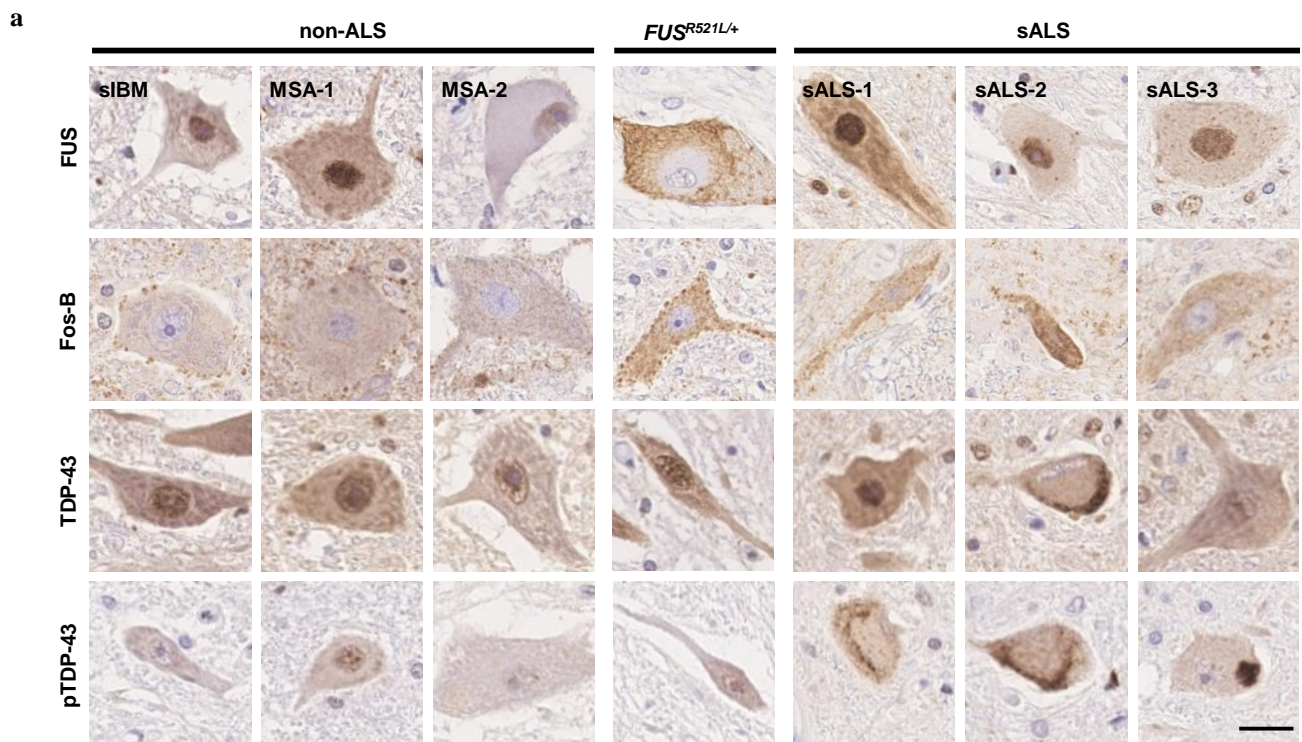relative length of axon / body length

Mock   hFos-B
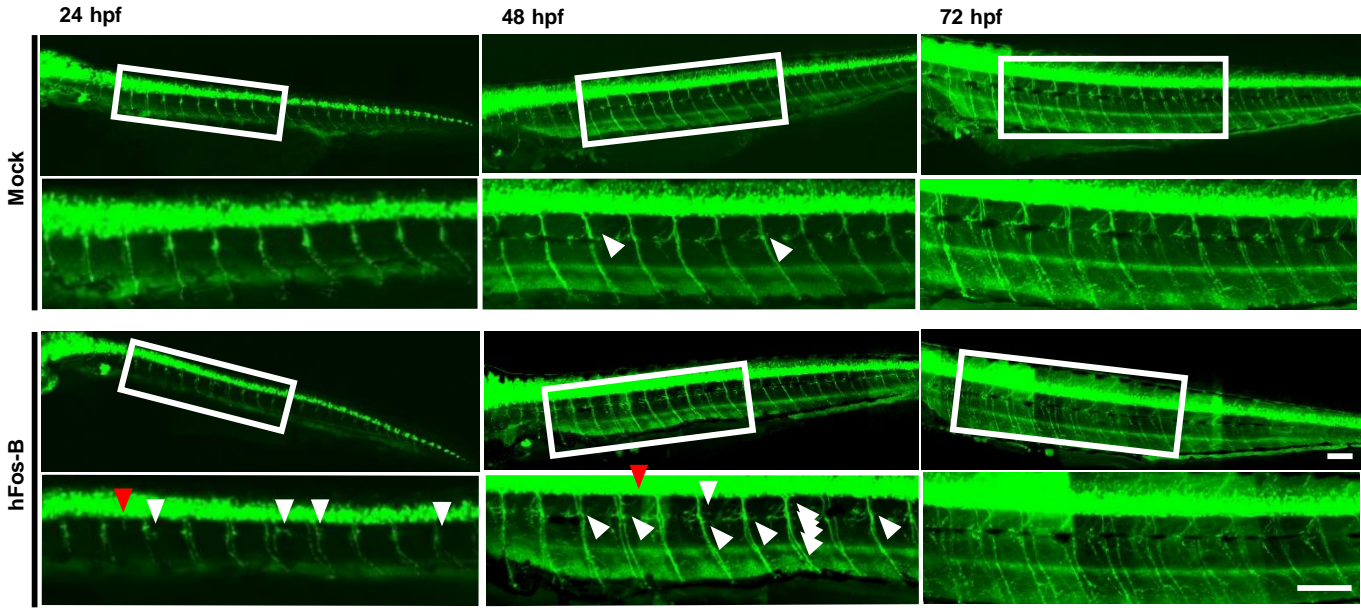
Supplementary Fig. 8. The *hFos-B* mRNA injection in *hb9:Venus* zebrafish.

(a–c) Abnormal increases in axon branching were confirmed with *hFos-B*-mRNA injection at 48 hpf. At 72 hpf, the axon branches were difficult to count because a considerable number of branches were detected at this time-point. a; Representative images of the zebrafish axons at 24, 48, and 72 hpf. Lower figures represent magnified images of the white squares of the upper figures. The abnormal spinal roots (red arrow heads) and axon branching (white arrowheads) increased in the *hFos-B* mRNA-injected line. Bar: 100 µm. b; The % of branching axons at 20 axons/line at 48 hpf. Axon branching significantly increased in the *hFos-B* mRNA-injected line. N = 3, Student's *t*-test. c; The degree of branching per axon at 20 axons/line at 48 hpf. Axon branching significantly increased in the *hFos-B* mRNA-injected line. N = 3, Student's *t*-test. (d) Quantification of axon length at 48 hpf. Axon length was adjusted with the spinal length. No differences in spinal length were observed between the two lines. N = 4, Student's *t* test.

Supplementary Figure 9

a

| | non-ALS | | | *FUS^R521L/+* | sALS | | |
| FUS | sIBM | MSA-1 | MSA-2 | | sALS-1 | sALS-2 | sALS-3 |

b

$p = 0.0029$
$p = 0.0056$
$p = 0.6725$

c

$r^2 = 0.160$
$r^2 = 0.008$
$r^2 = 0.220$

d

$r^2 = 0.102$
$r^2 = 0.509$
$r^2 = 0.058$

e

| Diagnosis | Fos-B upregulation | mis-localization of | | pTDP-43 deposit |
		FUS	TDP-43	
sIBM	-	-	-	-
MSA-1	-	-	-	-
MSA-1	-	-	-	-
FUS^R521L/+	+	+	-	-
sALS-1	±	-	-	+
sALS-2	+	-	+	+
sALS-3	-	-	-	+

Supplementary Fig. 9. Representative images of autopsied samples from all patients in the present study. (a) FUS was mislocalized from the nucleus to the cytoplasm only in $FUS^{R521L/+}$. Fos-B protein was overexpressed in the cytoplasm of ventral neurons of ALS patients with some variation. While pTDP-43 was aggregated in sALS cases, TDP-43 deposit was confirmed only in one case (sALS-2). Bar: 25 µm. (b) Quantification of the remnant anterior horn neurons in each group. Significant neuron loss was confirmed in patients with ALS, particularly in $FUS^{R521L/+}$ samples, as analyzed by one-way ANOVA. (c) Fos-B accumulation did not correlate with MN loss. Blue circles represent data from non-ALS samples. Pink circles represent data from sALS samples. Red circles represent data from $FUS^{R521L/+}$ samples. The regression lines of each dataset are presented along with the correlation coefficient (r^2). Black lines represent the regression line of all datasets, including non-ALS, sALS, and $FUS^{R521L/+}$. (d) There was no correlation between Fos-B upregulation and age at death. The scatter chart with the number of axon branching and age at autopsy are presented with the correlation coefficient (r^2). Black line represents the regression line of all datasets, including non-ALS, sALS, and $FUS^{R521L/+}$. (e) Inventory of protein abnormalities observed in this study. There was some variation in cytoplasmic pTDP-43 deposits and Fos-B upregulation.